Opto-Electronic Advances

Original Article

2022, Vol. 5, No. 5

DOI: 10.29026/oea.2022.200026

Parallel generation of low-correlation wideband complex chaotic signals using CW laser and external-cavity laser with self-phase-modulated injection

Anke Zhao, Ning Jiang*, Jiafa Peng, Shiqin Liu, Yiqun Zhang and Kun Qiu*

A novel scheme for generating optical chaos is proposed and experimentally demonstrated, which supports to simultaneously produce two low-correlation chaotic signals with wideband spectrum and suppressed time-delay-signature (TDS). In the proposed scheme, we use the output of an external-cavity semiconductor laser (ECSL) as the driving signal of a phase modulator to modulate the output of a CW laser. Then the phase-modulated continuous-wave (CW) light is split into two parts, one is injected back into the ECSL that outputs one chaotic signal, while the other part is passed through a dispersion module for generating another chaotic signal simultaneously. The experimental results prove that the proposed scheme has three merits. Firstly, it can improve the bandwidth of ECSL-based chaos by several times, and simultaneously generate another wideband flat-spectrum chaotic signal. Secondly, the undesired TDS characteristics of the simultaneously-generated chaotic signals can be efficiently suppressed to an indistinguishable level within a wide parameter range, as such the complexities of the chaotic signals are considerably high. Thirdly, the correlation coefficient between these two simultaneously-generated chaotic signals is smaller than 0.1. The proposed scheme provides an attractive solution for parallel multiple chaos generation, and shows great potential for multiple channel chaos communications and multiple random bit generations.

Keywords: optical chaos; optical feedback; semiconductor laser; electro-optic phase modulation

Zhao AK, Jiang N, Peng JF, Liu SQ, Zhang YQ et al. Parallel generation of low-correlation wideband complex chaotic signals using CW laser and external-cavity laser with self-phase-modulated injection. *Opto-Electron Adv* **5**, 200026 (2022).

Introduction

In the past two decades, optical chaos generation has been widely studied in several fields such as secure optical communication[1–6], physical random bit generation (RBG)[7–13], and optical logic[14]. In optical chaos communication systems, chaotic signal is used as the optical carrier to hide the message for enhancing the physical layer security. Recently, secure transmission of a 30 Gb/s data signal has been demonstrated in a 100-km fiber link, in which the bandwidth of the chaotic carrier is about 10 GHz[15]. Regarding to the chaos-based RBG, optical chaos is utilized as the physical source for extracting high-speed random bits by making use of its advantage of wide-spectrum characteristic, and the real-time RBG rate can be higher than Gb/s[7,10].

School of Information and Communication Engineering, University of Electronic Science and Technology of China, Chengdu 611731, China.

*Correspondence: N Jiang, E-mail: uestc_nj@uestc.edu.cn; K Qiu, E-mail: kqiu@uestc.edu.cn

Received: 8 July 2020; Accepted: 11 November 2020; Published online: 15 March 2022

Chaotic signals in the optical domain can be produced by semiconductor lasers (SLs), in virtue of various methods including optical feedback, optical injection, and electro-optical feedback[16]. Among these methods, external-cavity semiconductor laser (ECSL) with the optical feedback is the most extensively adopted configuration for its simplicity in structure and easy integration with optical chaos generator. However, in practical applications, the performance of ECSL is usually limited by two aspects: one is that the ECSL-generated chaos has an uneven power spectrum due to the intrinsic relaxation oscillation effect, which leads to a limited bandwidth of several GHz; the other is that the resonation of external cavity induces an undesired time-delay-signature (TDS), which degrades the randomness of obtained chaotic signal. Regarding the application in optical chaos communications, the limited bandwidth of chaotic carrier restricts the maximal data rate which can be encrypted, and the TDS affects the privacy of chaotic systems and finally degrade the system security. It has been proven that the TDS can be easily identified by several analysis methods, including autocorrelation function (ACF) and delayed mutual information (DMI)[17−20]. Once the eavesdropper knows the TDS of chaotic system, the ECSL system for chaotic carrier generation is highly risky to be reconstructed, and then the system security is threatened. Regarding the application in the chaos-based RBG, the limited bandwidth of the chaos source restricts the bit rate of RBG, and the TDS affects the randomness benchmark of the obtained bit sequence[10,21]. Therefore, it is of great significance to improve the bandwidth and conceal the TDS of ECSL-based chaotic signal.

In recent years, there are many methods which have been proposed for improving the effective bandwidth and suppressing the TDS characteristic of the ECSL-based chaotic signal. According to the literatures[22−28], there are generally two classes of methods which can suppress the TDS: one is using a complex optical feedback, such as double optical feedback[22], utilizing fiber grating as reflector[23,24], and introducing parallel-coupling ring resonators[25] into the optical feedback loop of conventional ECSL configuration; the other one is post-processing the ECSL output in virtue of nonlinear effects of optical fiber[26], delayed self-interface[27], and a compact phased array of semiconductor lasers[28]. Regarding the bandwidth enhancement of ECSL-based chaos, many techniques have also been proposed, such as heterodyning couplings[29,30], mutual injection[31], optical time lens[32], and self-phase-modulated feedback with phase-to-intensity conversion[33−35]. Nevertheless, in most of these schemes, only one single chaotic signal is generated, while simultaneous multiple chaos generation with low correlation is lack of study.

In this work, we propose and experimentally demonstrate a novel scheme for generating parallel wideband complex chaotic signals with low correlation, in virtue of constant-amplitude self-phase-modulation injection and phase-modulation to intensity-modulation conversion. With respect to the previously-reported chaos generation schemes, the proposed scheme can not only achieve bandwidth enhancement and TDS suppression for conventional ECSL-based chaotic signal, but also support to produce another wideband TDS-suppressed chaotic signal simultaneously. We experimentally realize the parallel generation of two flat-spectrum chaos which have an effective bandwidth of over 24 GHz and a high-complexity.

Experimental setup

Figure 1 presents the schematic diagram for the generation of parallel wideband complex chaotic signals. The output of a distributed-feedback (DFB) laser is equally split by a 3-dB fiber coupler (FC1) into two parts. One part is sent back into the DFB laser by the reflection of a mirror, to configurate a conventional ECSL system. A variable optical attenuator (VOA1) is deployed into the external cavity to tune the feedback strength. Here the definition of feedback strength is the power ratio of the optical feedback and the DFB emission. The other part is further split by FC2: one is referred to as the output-A of the system, while the other one is passed through VOA3 and then converted to an electronic chaos through a photodetector (PD3). The electronic chaos is subsequently passed through a radio-frequency (RF) amplifier and used as the driving signal of a phase modulator (PM). A CW light with a central wavelength of 1549.66 nm is used as the input light of the PM[36]. The linewidth and the emission power of the CW laser are 100 kHz and 8 dBm, respectively. The output of the PM is subsequently split by FC3: one part is injected to the DFB through the OC, while the other part propagates through a dispersion module (DM), and then is used as another chaotic output signal (referred to as the output-B) of the system. Here, we adopt a dispersion compensating fiber (DCF) as the DM, and the total dispersion value of the DCF is 342.3 ps/nm. The optical injection power of the

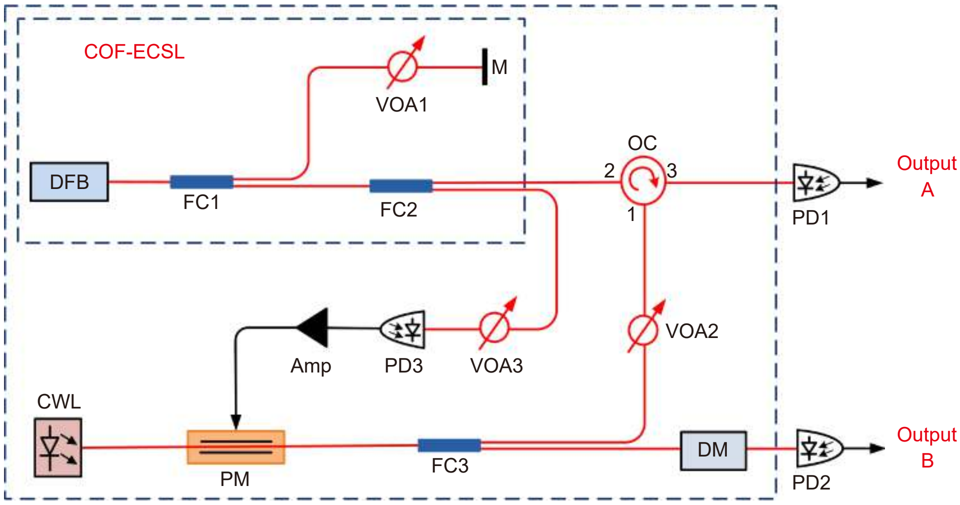

Fig. 1 | Experimental schematic diagram of the parallel wideband complex chaos generation. DFB, distributed-feedback laser; PM, electro-optic phase modulator; FC, fiber coupler; CWL, continuous-wave laser; PD, photodetector; M, mirror; VOA, variable optical attenuator; OC, optical circulator; Amp, radio-frequency amplifier; DM, dispersion module.

DFB is set to –3 dBm, which is controlled by VOA2. In our experiment, a current-temperature controller is used to control the emission power and the central wavelength of the DFB. The bias current of the DFB is set to 13.6 mA which corresponds to 1.5 times the threshold current, and operation wavelength is set to 1549.6 nm. The RF amplifier has a maximum power gain of 35 dB. The PM has a 3-dB bandwidth of 18 GHz and a half-wave voltage of 3.8 V. The maximum phase shift of the PM is about 1.5π, as the peak-to-peak values of the driving signal are 5.7 V. The splitting ratio of all the fiber couplers used in the experiment is 50∶50. A 25-GHz digital oscilloscope is used to measure and record the output signals, and its real-time sampling rate is set to 100 GS/s. In order to exhibit the properties of the scheme more intuitively, we compare the obtained chaotic signals in our scheme and the chaos obtained by a conventional optical feedback ECSL (COF-ECSL). The output of the COF-ECSL is obtained from the output-A without the injection from the CW laser.

Results and discussion

In Fig. 2, we present the time series and the power spectra for the chaotic output of the COF-ECSL (first column), and those of the chaos obtained by this scheme (second and third columns). Here, we choose the frequently-used effective bandwidth to evaluate the bandwidth characteristic of chaotic signals[29–35]. The power

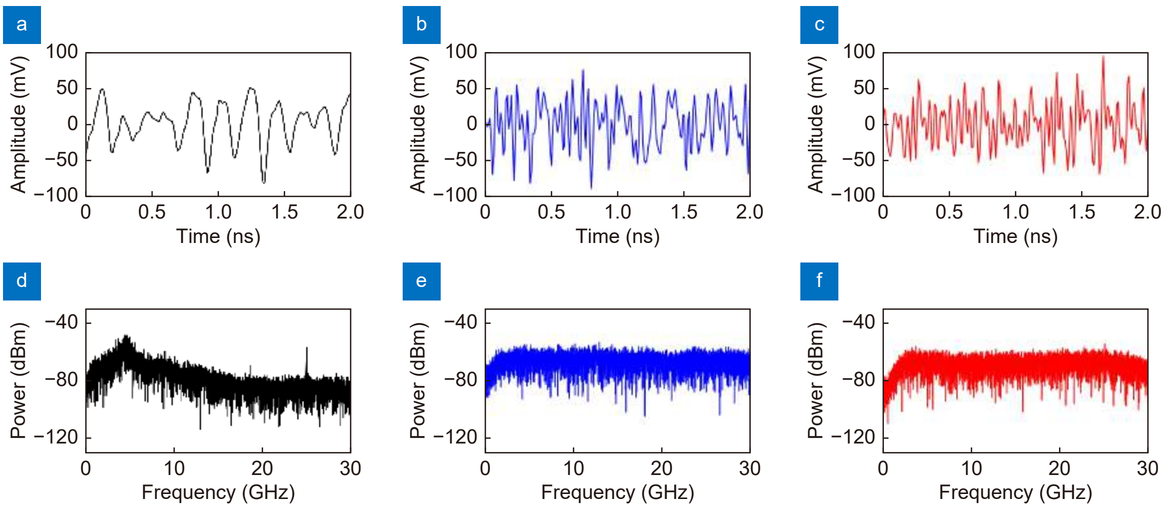

Fig. 2 | (**a**–**c**) Experimental time series and (**d**–**f**) power spectra of the chaotic signal obtained by the COF-ECSL (first column); those of the chaotic signals obtained from the output-A (second column), and the output-B of the proposed scheme (third column). The feedback strength is fixed to –30 dB.

spectra in frequency domain are derived by calculating the fast Fourier transformation of the digital signals measured by the oscilloscope. For the COF-ECSL-based chaos, as shown in Fig. 2(a) and 2(d), the power spectrum shows that most of the energy concentrates on the frequencies around laser relaxation oscillation (about 4.4 GHz) and degrades quickly as the frequency increases. Consequently, the corresponding effective bandwidth is only approximately 5.6 GHz. While for the two chaotic signals obtained in the proposed scheme, as illustrated in Fig. 2(e) and 2(f), the spectra are significantly broadened and much flatter than that of the COF-ECSL case. The effective bandwidths of the chaotic signals obtained from output-A and output-B are 24.2 GHz and 24.1 GHz, respectively, which are about four times larger than the value of the COF-ECSL-based chaos. The physical mechanism of the bandwidth enhancement is attributed to that, many new frequency components are generated by the phase modulation with chaotic driving signal, the spectrum of the CW light in optical domain is greatly expanded as proved in our previous work[35]. Then the DM and the DFB laser play the roles of nonlinear systems to convert the phase-modulation into intensity-modulation, and consequently the spectrum expansion in phase is converted to the bandwidth enhancement in intensity[36,37].

In Fig. 3, we present the influence of feedback strength on the behavior of the effective bandwidth. For the COF-ECSL-based chaos, the effective bandwidth slightly increases from 5.6 GHz to 7.5 GHz, with a variation of the feedback strength from −30 dB to −10 dB. In comparison, the effective bandwidths of the two wideband complex chaotic signals keep at a high level: the effective bandwidth of chaotic output-A slightly varies in the range from 23.9 GHz to 24.2 GHz, and that of chaotic output-B always maintains around 24 GHz with a small range of ±0.2 GHz. Thus, it can be concluded that our system can produce two parallel wideband chaotic signals within a wide feedback strength range, and the corresponding effective bandwidths can be maintained at several times larger than that of the COF-ECSL-based chaos. It is worth mentioning that, since the oscilloscope used in the experiment has a limited bandwidth of 25 GHz, the frequency components higher than 25 GHz are filtered and the calculated effective bandwidths of the two outputs maintain at a relatively fixed level. While the actual bandwidths of these chaotic signals may even be much larger than the measured values here, as we have confirmed in ref.[34,35].

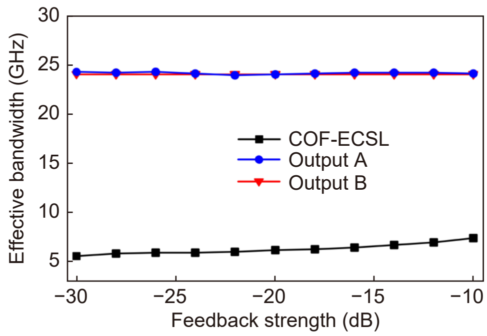

Fig. 3 | Effective bandwidths of the chaotic signals outputted by COF-ECSL (square), output-A (circle) and output-B (downward-triangle), as a function of feedback strength.

In order to investigate the properties of TDS suppression, Fig. 4 shows the ACF and DMI traces for the COF-ECSL-based chaos, the chaotic output-A and the chaotic output-B. A length of 2 μs is adopted for time series to

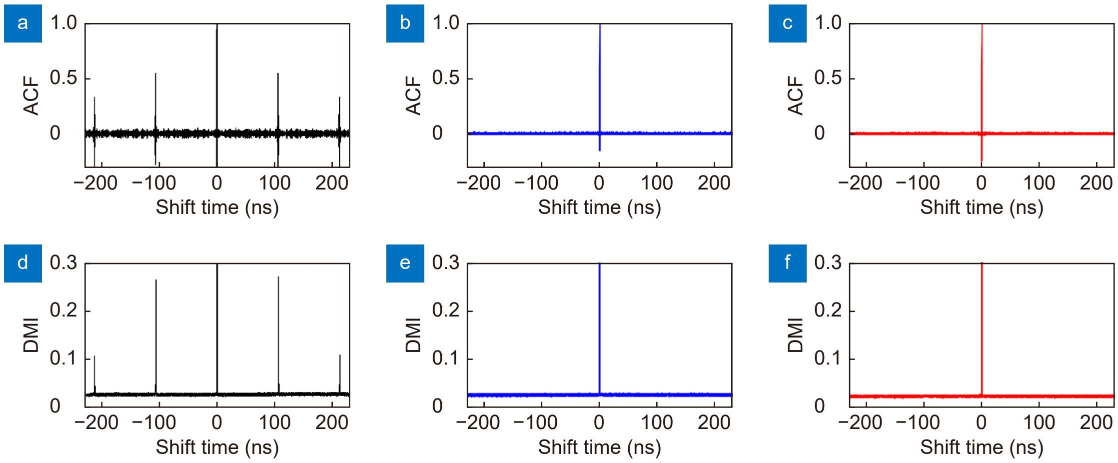

Fig. 4 | (**a–c**) ACF traces and (**d-f**) DMI traces of the chaos generated by COF-ECSL (first column), output-A (second column) and output-B (third column). The feedback strength is fixed to –30 dB.

calculate the ACF and DMI traces. For the COF-ECSL-generated chaos, large peaks are observed at the positions of the multiples of feedback delay as shown in Fig. 4(a) and 4(d), which suggests that the TDS can be easily exposed from the ACF and DMI traces. In comparison, for the chaos obtained in the proposed scheme (the second and third columns), no peaks can be identified at the position of the feedback delay in both of the ACF and DMI traces, indicating the TDS is significantly suppressed. The excellent TDS-concealment property in the proposed scheme can efficiently prevent the eavesdroppers from cracking the feedback delay time of chaotic system, as such the privacy of chaotic system for the chaos-based communication application can be greatly improved. Moreover, the suppression of TDS also enables the feedback delay of chaotic systems to be used as a hardware key to further enlarge the key space of chaos-based communication systems. In addition, since the ACF traces of the two outputs have no side peaks, the proposed chaos generation system can also be applied as an excellent physical source for the application in LiDAR[40].

Figure 5 shows the influence of feedback strength on the behavior of TDS suppression. The TDS values are evaluated by the maximum values in the vicinity of the position of feedback delay in the ACF and DMI traces. Under the scenario of COF-ECSL, the evolution trends of TDS values in the ACF and DMI traces are similar, which show that the TDS values firstly decrease and then gradually increase, with the increase of feedback strength. The TDS values in this scenario are always larger than 0.1, which are easy to be identified from the ACF and DMI traces. While in the proposed scheme, for both of the two chaotic outputs, the TDS values are smaller than 0.02 as we increase the feedback strength from −30 dB to −10 dB. The results indicate that the TDS can be perfectly concealed within a large range of feedback strength.

Complexity of chaos is another important indicator which would affect the security of optical chaos communication and the randomness of chaos-based RBG, thus we investigate the complexities of the generated wideband TDS-suppressed chaotic signals versus the feedback strength in Fig. 6. To evaluate the extent of disorder in a chaotic signal, the permutation entropy (PE) is calculated to quantify the complexity of chaos[3,19,38,39]. The time series with a length of 2×10^5 are adopted for calculating the value of PE. The embedding dimension is 5 and the embedding delay $\tau = f_s \cdot \tau_f$ (where τ_f is the feedback delay time and f_s is the sampling frequency). The larger PE value means the higher complexity of chaos (the maximum value is 1). The calculated PE value of the chaos generated by the COF-ECSL firstly increases gradually from 0.939, then reaches at a maximum value of 0.979, and after that, it slightly degrades, as the feedback strength increases from −30 dB to −10 dB. While the PE values of the two wideband chaotic outputs are always larger than that in the COF-ECSL scenario. The PE values of the output A and output B maintain at a stable level of 0.998. Therefore, the complexities of the generated wideband chaotic signals are significantly enhanced by the proposed scheme in comparison with that of the COF-ECSL scenario. Moreover, since the PE values of the output A and output B are close to 1, the complexities of these two outputs are close to the ideal noise level (PE=1). The excellent complexity-enhancement property is beneficial to enhance the system security for the application of chaos communications and improve the bit randomness of RBG application.

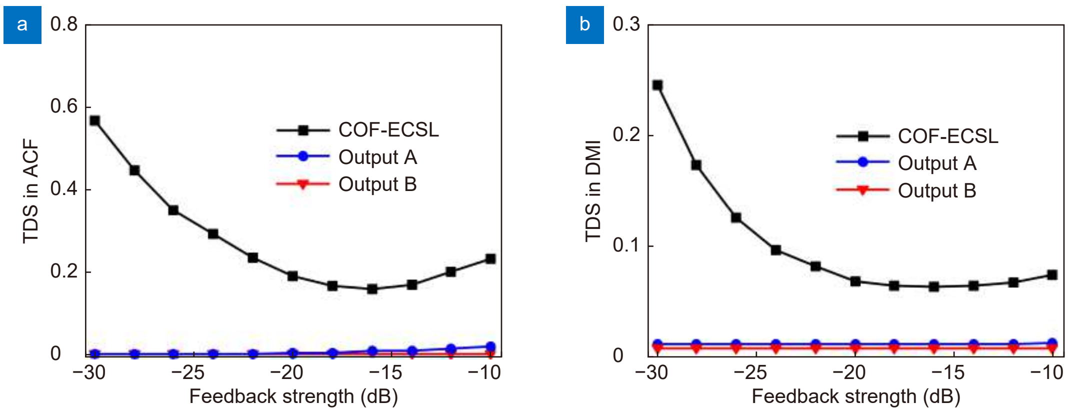

Fig. 5 | |TDS values in (**a**) ACF traces and (**b**) DMI traces of the chaos generated by COF-ECSL (square), output-A (circle) and output-B (downward-triangle), as a function of feedback strength.

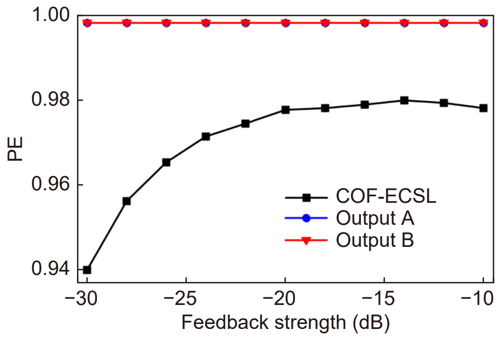

Fig. 6 | PE values of the chaos obtained by the COF-ECSL (square), the output-A (circle) and the output-B (downward-triangle), as a function of the feedback strength.

In the proposed system, the output A is used as the driving signal of the PM, and the output B is originated from the phase-modulated light after passing through the DM, the two chaotic outputs are related to each other in structure. Next, we investigate the cross-correlation between these simultaneously-generated chaotic signals. The cross-correlation coefficient (CC) is adopted to evaluate their correlation, which is defined as[4,15]:

$$CC = \frac{\langle (I_1(t) - \langle I_1(t)\rangle) \cdot (I_2(t) - \langle I_2(t)\rangle)\rangle}{\sqrt{\langle (I_1(t) - \langle I_1(t)\rangle)^2\rangle \langle (I_2(t) - \langle I_2(t)\rangle)^2\rangle}} , \quad (1)$$

where $I_1(t)$ and $I_2(t)$ are the experimental time domain signals, and <·> is the time averaging. The subscripts 1, 2 correspond to the two temporal chaotic waveforms of output-A and output-B, respectively. In Fig. 7, we present the influence of the feedback strength on the cross correlation. It can be seen that the CC slightly decreases and maintains at a low level smaller than 0.1 as the feedback strength exceeds −30 dB. The small variation of the CC trend is because that the increasing feedback strength would induce a larger intensity fluctuation for the chaotic driving signal of phase modulator. The insets illustrate the time series of chaotic signals obtained from output-A (blue line) and output-B (red line) in different feedback strengths cases, which show that the intensity fluctuations under these exemplary cases are completely different. The results indicate that the two generated chaotic signals in the proposed scheme have low correlation, which is beneficial to various chaos-based applications. For example, in the application of chaos-based optical communications, the proposed scheme can simultaneously provide two low-correlation chaotic carriers to encrypt the messages from two different channels, and consequently the transmission capacity can be enhanced by two times. On the other hand, in the application of chaos-based RBG, the proposed system can provide two independent wideband physical entropy sources, which can be utilized to extract two independent ultrafast random bit sequences simultaneously, as such the total bit rate of RBG can be also improved.

In addition, Fig. 8 presents the time series and the corresponding probability distribution functions of the chaotic signal generated by the COF-ECSL, as well as those of the two outputs in the proposed scheme. It is demonstrated that the amplitude distributions of the output A and output B approach the Gaussian distribution, which are much more symmetrical than the COF-ECSL-based chaotic output. The symmetrical

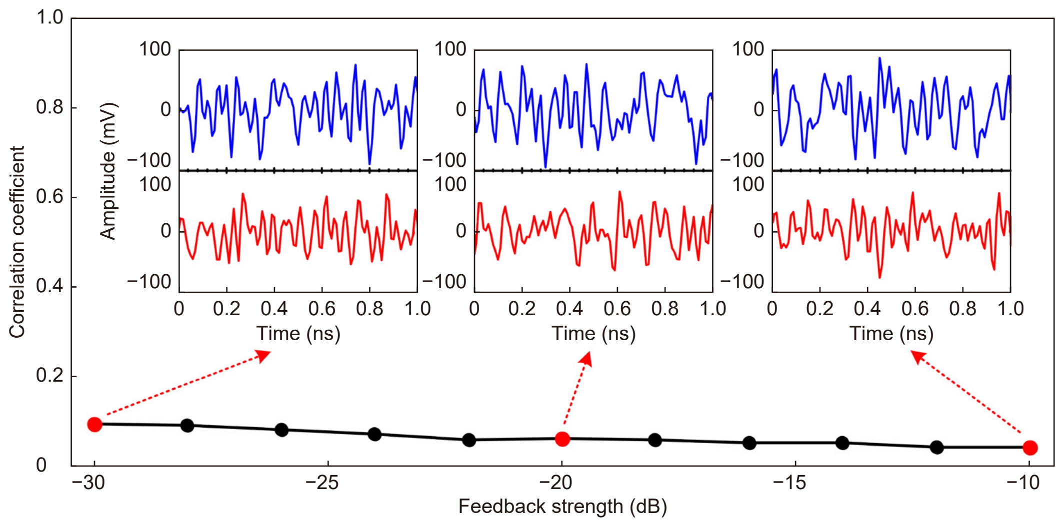

Fig. 7 | Correlation coefficient between chaotic signals obtained from output-A and output-B, as a function of feedback strength. The insets are the temporal waveforms of the two chaotic outputs (with a range of 1 ns) measured at the feedback strengths of –30 dB, –20 dB and –10 dB, respectively.

distributions further confirm the randomness and complexity enhancement of the output signals in the proposed scheme, which are also highly beneficial to achieving nearly equal numbers of ones and zeros in random bit generation[11,12].

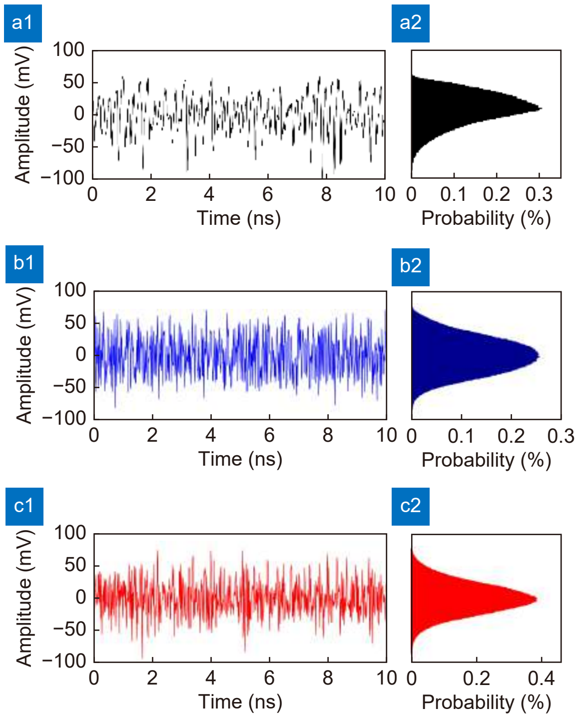

Fig. 8 | Experimental time series (left column) and amplitude probability distributions (right column) of (**a**) the chaos generated by the COF-ECSL, as well as (**b**) the chaotic output-A and (**c**) the chaotic output-B of the proposed scheme.

Conclusions

In this paper, a novel parallel wideband complex chaos generation scheme is experimentally demonstrated, by introducing the constant-amplitude self-phase-modulation injection into an ECSL and applying the phase-to intensity conversion of a dispersive device into the phase-modulated CW light. The proposed scheme can not only achieve the bandwidth enhancement and TDS suppression of the ECSL-based chaos, but also simultaneously generate another wideband TDS-suppressed chaotic signal. It is indicated that two simultaneously-generated chaotic signals with effective bandwidths around 24 GHz can be easily obtained, and the effective bandwidth can be always maintained at several times larger than that of the conventional ECSL-generated chaos. Moreover, the TDS characteristics of the simultaneously-generated chaotic signals are completely concealed at an indistinguishable level (<0.02) within a large feedback strength range. As a result, the complexities of the generated chaotic signals are considerably high and approaching to that of an ideal random noise. In addition, the experimental results also show that the correlation between these two simultaneously-generated chaos is low with a CC value smaller than 0.1. The proposed scheme paves a novel way for generating parallel multiple low-correlation chaotic signals, which has great potential for various chaos-based application, such as multi-channel secure optical communications and parallel ultrafast random bit generations.

References

1. Argyris A, Syvridis D, Larger L, Annovazzi-Lodi V, Colet P et al. Chaos-based communications at high bit rates using commercial fibre-optic links. *Nature* **438**, 343–346 (2005).
2. Ke JX, Yi LL, Yang Z, Yang YP, Zhuge QB et al. 32 Gb/s chaotic optical communications by deep-learning-based chaos synchronization. *Opt Lett* **44**, 5776–5779 (2019).
3. Fu YD, Cheng MF, Jiang XX, Yu Q, Huang LBJ et al. High-speed optical secure communication with an external noise source and an internal time-delayed feedback loop. *Photon Res* **7**, 1306–1313 (2019).
4. Deng T, Xia GQ, Wu ZM. Broadband chaos synchronization and communication based on mutually coupled VCSELs subject to a bandwidth-enhanced chaotic signal injection. *Nonlinear Dyn* **76**, 399–407 (2014).
5. Jiang N, Zhao AK, Xue CP, Tang JM, Qiu K. Physical secure optical communication based on private chaotic spectral phase encryption/decryption. *Opt Lett* **44**, 1536–1539 (2019).
6. Li NQ, Susanto H, Cemlyn B, Henning ID, Adams MJ. Secure communication systems based on chaos in optically pumped spin-VCSELs. *Opt Lett* **42**, 3494–3497 (2017).
7. Uchida A, Amano K, Inoue M, Hirano K, Naito S et al. Fast physical random bit generation with chaotic semiconductor lasers. *Nat Photon* **2**, 728–732 (2008).
8. Tang X, Wu ZM, Wu JG, Deng T, Chen JJ et al. Tbits/s physical random bit generation based on mutually coupled semiconductor laser chaotic entropy source. *Opt Express* **23**, 33130–33141 (2015).
9. Li XZ, Li SS, Zhuang JP, Chan SC. Random bit generation at tunable rates using a chaotic semiconductor laser under distributed feedback. *Opt Lett* **40**, 3970–3973 (2015).
10. Li P, Zhang JG, Sang LX, Liu XL, Guo YQ et al. Real-time online photonic random number generation. *Opt Lett* **42**, 2699–2702 (2017).
11. Reidler I, Aviad Y, Rosenbluh M, Kanter I. Ultrahigh-speed random number generation based on a chaotic semiconductor laser. *Phys Rev Lett* **103**, 024102 (2009).
12. Kanter I, Aviad Y, Reidler I, Cohen E, Rosenbluh M. An optical ultrafast random bit generator. *Nat Photon* **4**, 58–61 (2010).
13. Zhao AK, Jiang N, Wang YJ, Liu SQ, Li BC et al. Correlated random bit generation based on common-signal-induced synchronization of wideband complex physical entropy sources. *Opt Lett* **44**, 5957–5960 (2019).
14. Xiang SY, Ren ZX, Zhang YH, Song ZW, Hao Y. All-optical

neuromorphic XOR operation with inhibitory dynamics of a single photonic spiking neuron based on a VCSEL-SA. *Opt Lett* **45**, 1104–1107 (2020).
15. Ke JX, Yi LL, Xia GQ, Hu WS. Chaotic optical communications over 100-km fiber transmission at 30-Gb/s bit rate. *Opt Lett* **43**, 1323–1326 (2018).
16. Sciamanna M, Shore KA. Physics and applications of laser diode chaos. *Nat Photon* **9**, 151–162 (2015).
17. Rontani D, Locquet A, Sciamanna M, Citrin DS, Ortin S. Time-delay identification in a chaotic semiconductor laser with optical feedback: a dynamical point of view. *IEEE J Quantum Electron* **45**, 879–1891 (2009).
18. Xiang SY, Pan W, Luo B, Yan LS, Zou XH et al. Wideband unpredictability-enhanced chaotic semiconductor lasers with dual-chaotic optical injections. *IEEE J Quantum Electron* **48**, 1069–1076 (2012).
19. Zhang LY, Pan W, Yan LS, Luo B, Zou XH et al. Isochronous cluster synchronization in delay-coupled VCSEL networks subjected to variable-polarization optical injection with time delay signature suppression. *Opt Express* **27**, 33369–33377 (2019).
20. Li NQ, Pan W, Locquet A, Citrin DS. Time-delay concealment and complexity enhancement of an external-cavity laser through optical injection. *Opt Lett* **40**, 4416–4419 (2015).
21. Sakuraba R, Iwakawa K, Kanno K, Uchida A. Tb/s physical random bit generation with bandwidth-enhanced chaos in three-cascaded semiconductor lasers. *Opt Express* **23**, 1470–1490 (2015).
22. Wu JG, Xia GQ, Wu ZM. Suppression of time delay signatures of chaotic output in a semiconductor laser with double optical feedback. *Opt Express* **17**, 20124–20133 (2009).
23. Zhong ZQ, Wu ZM, Xia GQ. Experimental investigation on the time-delay signature of chaotic output from a 1550 nm VCSEL subject to FBG feedback. *Photon Res* **5**, 6–10 (2017).
24. Wang DM, Wang LS, Zhao T, Gao H, Wang YC et al. Time delay signature elimination of chaos in a semiconductor laser by dispersive feedback from a chirped FBG. *Opt Express* **25**, 10911–10924 (2017).
25. Jiang N, Wang YJ, Zhao AK, Liu SQ, Zhang YQ et al. Simultaneous bandwidth-enhanced and time delay signature-suppressed chaos generation in semiconductor laser subject to feedback from parallel coupling ring resonators. *Opt Express* **28**, 1999–2009 (2020).
26. Li SS, Li XZ, Chan SC. Chaotic time-delay signature suppression with bandwidth broadening by fiber propagation. *Opt Lett* **43**, 4751–4754 (2018).
27. Wang AB, Yang YB, Wang BJ, Zhang BB, Li L et al. Generation of wideband chaos with suppressed time-delay signature by delayed self-interference. *Opt Express* **21**, 8701–8710 (2013).
28. Zhou P, Fang Q, Li NQ. Phased-array assisted time-delay signature suppression in the optical chaos generated by an external-cavity semiconductor laser. *Opt Lett* **45**, 399–402 (2020).
29. Xiang SY, Wen AJ, Pan W, Lin L, Zhang HX et al. Suppression of chaos time delay signature in a ring network consisting of three semiconductor lasers coupled with heterogeneous delays. *J Lightware Technol* **34**, 4221–4227 (2016).
30. Cheng CH, Chen YC, Lin FY. Chaos time delay signature suppression and bandwidth enhancement by electrical heterodyning. *Opt Express* **23**, 2308–2319 (2015).
31. Qiao LJ, Lv TS, Xu Y, Zhang MJ, Zhang JZ et al. Generation of flat wideband chaos based on mutual injection of semiconductor lasers. *Opt Lett* **44**, 5394–5397 (2019).
32. Jiang N, Wang C, Xue CP, Li GL, Lin SQ et al. Generation of flat wideband chaos with suppressed time delay signature by using optical time lens. *Opt Express* **25**, 14359–14367 (2017).
33. Jiang N, Zhao AK, Liu SQ, Xue CP, Wang BY et al. Generation of broadband chaos with perfect time delay signature suppression by using self-phase-modulated feedback and a microsphere resonator. *Opt Lett* **43**, 5359–5362 (2018).
34. Zhao AK, Jiang N, Liu SQ, Xue CP, Tang JM et al. Wideband complex-enhanced chaos generation using a semiconductor laser subject to delay-interfered self-phase-modulated feedback. *Opt Express* **27**, 12336–12348 (2019).
35. Zhao AK, Jiang N, Liu SQ, Xue CP, Qiu K. Wideband time delay signature-suppressed chaos generation using self-phase-modulated feedback semiconductor laser cascaded with dispersive component. *J Lightwave Technol* **37**, 5132–5139 (2019).
36. Zhao AK, Jiang N, Chang CC, Wang YJ, Liu SQ et al. Generation and synchronization of wideband chaos in semiconductor lasers subject to constant-amplitude self-phase-modulated optical injection. *Opt Express* **28**, 13292–13298 (2020).
37. Zhao ZX, Cheng MF, Luo CK, Deng L, Zhang MM et al. Synchronized random bit sequences generation based on analog-digital hybrid electro-optic chaotic sources. *J Lightw Technol* **36**, 4995–5002 (2018).
38. Hong YH, Ji SK. Effect of digital acquisition on the complexity of chaos. *Opt Lett* **42**, 2507–2510 (2017).
39. Cheng MF, Luo CK, Jiang XX, Deng L, Zhang MM et al. An electrooptic chaotic system based on a hybrid feedback loop. *J Lightwave Technol* **36**, 4259–4266 (2018).
40. Liu B, Yu Y, Chen Z, Han WQ. True random coded photon counting Lidar. *Opto-Electron Adv* **3**, 190044 (2020).

Acknowledgements

This work was supported by the National Natural Science Foundation of China (Grant no. 62171087, 61671119), the Sichuan Science and Technology Program (Grant no. 2021JDJQ0023), and the Fundamental Research Funds for the Central Universities (Grant no. ZYGX2019J003).

Author contributions

A. K. Zhao and N. Jiang proposed the original idea and perform the experiment; J. F Peng, S. Q. Liu and Y. Q. Zhang contributed to analysis and manuscript preparation; K. Qiu helped perform the analysis with constructive discussions.

Competing interests

The authors declare no competing financial interests.